Article

Near-Infrared Light Activated Release of Nitric Oxide from Designed Photoactive Manganese Nitrosyls: Strategy, Design, and Potential as NO Donors

Aura A. Eroy-Reveles, Yvonne Leung, Christine M. Beavers, Marilyn M. Olmstead, and Pradip K. Mascharak

J. Am. Chem. Soc., **2008**, 130 (13), 4447-4458 • DOI: 10.1021/ja710265j

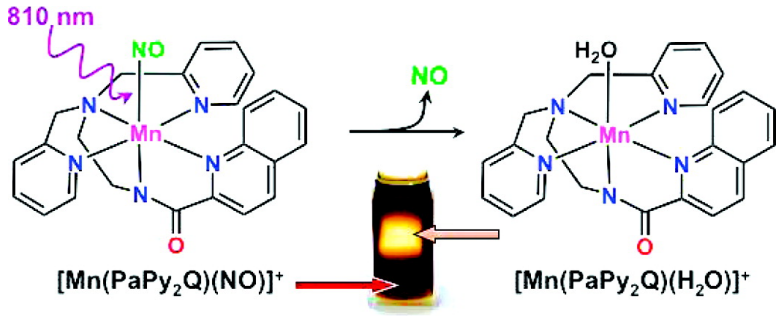

More About This Article

Additional resources and features associated with this article are available within the HTML version:

- Supporting Information
- Links to the 2 articles that cite this article, as of the time of this article download
- Access to high resolution figures
- Links to articles and content related to this article
- Copyright permission to reproduce figures and/or text from this article

View the Full Text HTML

J|A|C|S
ARTICLES
Published on Web 03/12/2008

Near-Infrared Light Activated Release of Nitric Oxide from Designed Photoactive Manganese Nitrosyls: Strategy, Design, and Potential as NO Donors

Aura A. Eroy-Reveles, Yvonne Leung, Christine M. Beavers, Marilyn M. Olmstead, and Pradip K. Mascharak*

Department of Chemistry and Biochemistry, University of California, Santa Cruz, California 95064, and the Department of Chemistry, University of California, Davis, California, California 95616

Received November 12, 2007; E-mail: pradip@chemistry.ucsc.edu

Abstract: Two new manganese complexes derived from the pentadentate ligand *N*,*N*-bis(2-pyridylmethyl)-amine-*N*-ethyl-2-quinoline-2-carboxamide, $PaPy_2QH$, where H is dissociable proton), namely, $[Mn(PaPy_2Q)(NO)]ClO_4$ (**2**) and $[Mn(PaPy_2Q)(OH)]ClO_4$ (**3**), have been synthesized and structurally characterized. The Mn(III) complex $[Mn(PaPy_2Q)(OH)]ClO_4$ (**3**), though insensitive to dioxygen, reacts with nitric oxide (NO) to afford the nitrosyl complex $[Mn(PaPy_2Q)(NO)]ClO_4$ (**2**) via reductive nitrosylation. This diamagnetic $\{Mn\text{-}NO\}^6$ nitrosyl exhibits ν_{NO} at 1725 cm^{-1} and is highly soluble in water, with λ_{max} at 500 and 670 nm. Exposure of solutions of **2** to near-infrared (NIR) light (810 nm, 4 mW) results in bleaching of the maroon solution and detection of free NO by an NO-sensitive electrode. The quantum yield of **2** ($\Phi = 0.694 \pm 0.010$, $\lambda_{irr} =$ 550 nm, H_2O) is much enhanced over the first generation $\{Mn\text{-}NO\}^6$ nitrosyl derived from analogous polypyridine ligand, namely, $[Mn(PaPy_3)(NO)]ClO_4$ (**1**, $\Phi = 0.385 \pm 0.010$, $\lambda_{irr} = 550$ nm, H_2O), reported by this group in a previous account. Although quite active in the visible range (500−600 nm), **1** exhibits very little photoactivity under NIR light. Both **1** and **2** have been incorporated into sol−gel (SG) matrices to obtain nitrosyl−polymer composites **1·SG** and **2·SG**. The NO-donating capacities of the polyurethane-coated hybrid materials **1·HM** and **2·HM** have been determined. **2·HM** has been used to transfer NO to reduced myoglobin with 780 nm light. The various strategies for synthesizing photosensitive metal nitrosyls have been discussed to establish the merits of the present approach. The results of the present study confirm that proper ligand design is a very effective way to isolate photoactive manganese nitrosyls that could be used to deliver NO to biological targets under the control of NIR light.

Introduction

In recent years, nitric oxide (NO) has been recognized as a key mediator in a diverse array of physiological and pathological responses.[1] This odd-electron diatomic gaseous molecule, produced endogenously by nitric oxide synthase (NOS), acts as a signaling molecule to regulate blood pressure, neurotransmission, inhibition of platelet aggregation, cell-mediated immune response, antimicrobial activity, and cell death.[2] The biological activity of NO depends heavily on the dose and duration of exposure, as well as on the cellular sensitivity to NO. For example, relatively low concentrations (2 to 300 nM) of NO produced by the constitutive isoforms of NOS (nNOS and eNOS) are required for its neurological and vascular function.[3] Much larger concentrations (low mM) of NO, such as those produced by activated macrophages via the inducible isoform of NOS (iNOS), however, lead to cytotoxicity.[4,5] Furthermore, inhibition of respiratory complexes, DNA damage and modification, gene mutation, and cell apoptosis can all be induced by high doses of NO, resulting in tumor regression and inhibition of metastasis.[6]

The discovery of the tumorcidal properties of NO has raised interest in the development of compounds that are capable of

(1) (a) *Nitric Oxide: Novel Actions, Deleterious Effects, and Clinical Potential*; Chiueh, C. C., Hong, J.-S., Leong, S. K., Eds.; New York Academy of Sciences: New York, 2002; p 962. (b) *Nitric Oxide: Biology and Pathology*; Ignarro, L. J., Ed.; Academic Press: San Diego, 2000. (c) Fukuto, J. M.; Wink, D. A. *Metal Ions Biol. Syst.* **1999**, *36*, 547−595. (d) Lincoln, J.; Burnstock, G. *Nitric Oxide in Health and Disease*; Cambridge University Press: New York, 1997. (e) *Methods in Nitric Oxide Research*; Feelisch, M., Stamler, J. S., Eds.; J. Wiley and Sons: Chichester, England, 1996. (f) Weissman, B. A.; Allan, N.; Shapiro, S. *Biochemical, Pharmacological, and Clinical Aspects of Nitric Oxide*; Plenum Press: New York, 1995. (g) Butler, A. R.; Williams, D. L. H. *Chem. Soc. Rev.* **1993**, *22*, 223−241.

(2) (a) Kalsner, S. *Nitric Oxide and Free Radicals in Peripheral Neurotransmission*; Birkhäuser: Boston, 2000. (b) *Nitric Oxide and Infection*; Fang, F. C., Ed.; Kluwer Academic/Plenum Publishers: New York, 1999. (c) *Nitric Oxide and the Cell: Proliferation, Differentiation and Death*; Moncada, S., Higgs, E. A., Bagetta, G., Eds.; Portland Press: London, 1998. (d) *Nitric Oxide and the Kidney*; Goligorsky, M. S., Gross, S. S., Eds.; Chapman & Hall: New York, 1997. (e) *Nitric Oxide: Principles and Actions*; Lancaster, J., Jr., Ed.; Academic Press: San Diego, 1996. (f) Zhang, J.; Snyder, S. H. *Annu. Rev. Pharmacol. Toxicol.* **1995**, *19*, 711−721. (g) Schmidt, H. H. H. W.; Walter, U. *Cell* **1994**, *78*, 919−925.

(3) Li, T.; Poulos, T. L. *J. Inorg. Biochem.* **2005**, *99*, 293−305. (b) Rosen, G. M.; Tsai, P.; Pou, S. *Chem. Rev.* **2002**, *102*, 1191−1199. (c) Forstermann, U.; Boissel, J. P.; Kleinert, H. *FASEB J.* **1998**, *12*, 773−790.

(4) (a) Brüne, B. *Cell Death Diff.* **2003**, *10*, 864−869. (b) Ishiropoulos, H.; Zhu, L.; Beckman, J. S. *Arch. Biochem. Biophys.* **1992**, *298*, 446−451.

(5) (a) Fukumura, D.; Kashiwagi, S.; Jain, R. K. *Nat. Rev. Cancer* **2006**, *6*, 521−534. (b) Taylor, E. L.; Megson, I. L.; Haslett, C.; Rossi, A. G. *Cell Death Differ.* **2003**, *10*, 418−430.

delivering NO (NO donors) on demand.[7] To date, a variety of NO donors, both organic and metal-based, have been synthesized. These exogenous NO sources release NO via enzymatic pathways as well as by stimuli such as change in pH, heat, and light.[8] Among the organic NO donors, selected diazeniumdiolates (NONOates) and *S*-nitrosothiols (such as *S*-nitrosoglutathione **(**GSNO) and *S*-nitroso-*N*-acetylpenicillamine SNAP) have been shown to induce apoptosis in a variety of cell types.[9,10] NO donors that release NO photochemically have generated much interest because they allow localized release of NO and could be used for photodynamic therapy (PDT) of cancer cells.[11,12] It has been demonstrated that cells subjected to PDT produce NO.[13] Because NO reacts with various reactive oxygen species generated by PDT, it has been suggested that NO contributes to the effective outcome of PDT treatment.[14] In recent years, interest in metal NO complexes (nitrosyls) has been renewed following the successful use of sodium nitroprusside ($Na_2[Fe(CN)_5NO]$, SNP) as a NO donor drug to control blood pressure during hypertensive episodes.[15] Interestingly, nitrosyls like SNP and Roussin's salts (iron−sulfur clusters that store multiple equivalents of NO) release NO upon illumination with light (300−500 nm).[16,17] However, low quantum yields (Φ) and problems associated with ancillary ligands (such as cyanide in case of SNP) limit the use of such nitrosyls in PDT.[18]

We have recently focused our attention on designed metal nitrosyls that rapidly release NO upon illumination with low-intensity light of low frequency.[19−29] In such attempts, we have employed nonporphyrin polydentate ligands[30] to avoid problems associated with rapid NO recombination reactions (commonly observed with metal nitrosyls derived from porphyrin ligands)[31,32] and toxicity arising from ancillary ligands.[17] Careful consideration of several metric, spectroscopic, and redox parameters (as discussed in our previous papers) led us to the designed ligand $PaPy_3H$ (*N*,*N*-bis(2-pyridylmethyl)amine-*N*-ethyl-2-pyridine-2-carboxamide). This pentadentate ligand allowed us to synthesize the first non-heme diamagnetic {Fe−NO}^{6} nitrosyl[33] $[Fe(PaPy_3)(NO)](ClO_4)_2$ that rapidly releases NO upon illumination with 5−10 mW of *visible* light (500−600 nm) in solvents like acetonitrile ($\Phi = 0.18$).[19,20] Our results strongly suggest that the presence of the deprotonated carboxamido nitrogen (a strong σ-donating negatively charged donor) *trans* to the bound NO in this nitrosyl is crucial for its photolability.[21] Although $[Fe(PaPy_3)(NO)](ClO_4)_2$ exhibits excellent NO photolability, its stability in biological media is inadequate.[22,23] To circumvent this problem, we next synthesized the corresponding ruthenium nitrosyl, namely, $[Ru(PaPy_3)(NO)](BF_4)_2$.[24] This nitrosyl is soluble in water and very stable in aqueous solution (pH range 5−9), a prerequisite for biological use. Indeed, we have employed this nitrosyl to deliver NO to biological targets such as reduced myoglobin and cytochrome *c* oxidase.[24,34] This success, however, came with a compromise. $[Ru(PaPy_3)(NO)](BF_4)_2$ releases NO only when exposed to low-intensity UV light (5−10 mW, 300−450 nm); no appreciable NO photolability is observed with visible light. Although the intensity of UV light required for NO photolability is very low for $[Ru(PaPy_3)(NO)](BF_4)_2$ compared to other UV-sensitive ruthenium nitrosyls,[35,36] the need for an efficient NO donor that operates under visible light remained open. The quest came to a decent stop when we synthesized the manganese nitrosyl, $[Mn(PaPy_3)(NO)]ClO_4$ (**1**).[28] This {Mn−NO}^{6} nitrosyl is stable in aqueous buffer and rapidly releases NO when exposed to *visible* light (500−650 nm), affording the Mn(II) aqua species $[Mn(PaPy_3)(H_2O)]ClO_4$. We have been able to employ **1** as a photosensitive NO donor

(6) (a) Simeone, A.-M.; Collela, S.; Krahe, R.; Johnson, M. M.; Mora, E.; Tari, A. M. *Carcinogenesis* **2006**, *27*, 568−577. (b) Crowell, J. A.; Steele, V. E.; Sigman, C. C.; Fay, J. R. *Mol. Cancer Ther.* **2003**, *2*, 815−823. (c) Hobbs, A. J.; Higgs, A.; Moncada, S. *Ann. Rev. Pharmacol. Toxicol.* **1999**, *39*, 191−220. (d) Brüne, B.; von Knethen, A.; Sandau, K. *Eur. J. Pharmacol.* **1998**, *351*, 261−272.

(7) (a) Thatcher, G. R. J. *Curr. Top. Med. Chem.* **2005**, *5*, 597−601. (b) Napoli, C.; Ignarro, L. J. *Annu. Rev. Pharmacol. Toxicol.* **2003**, *43*, 97−123. (c) Feelish, M. *Naunyn-Schmiedeberg's Arch. Pharmacol.* **1998**, *358*, 113−122. (d) Keefer, L. K.; Nims, R. W.; Davies, K. M.; Wink, D. A. *Methods Enzymol.* **1996**, *268*, 281−293.

(8) (a) *Nitric Oxide Donors*; Wang, P. G., Cai, T. B., Taniguchi, N., Eds.; Wiley: Weinheim, Germany, 2005. (b) Wang, P. G.; Xian, M.; Tang, X.; Wu, X.; Wen, Z.; Cai, T.; Janczuk, A. J. *Chem. Rev.* **2002**, *102*, 1091−1134.

(9) (a) Keefer, L. K. *Curr. Top. Med. Chem.* **2005**, *5*, 625−636. (b) Keefer, L. K. *Annu. Rev. Pharmacol. Toxicol.* **2003**, *43*, 585−607.

(10) (a) Jekabsone, A.; Dapkunas, Z.; Brown, G. C.; Borutaite, V. *Biochem. Pharmacol.* **2003**, *66*, 1513−1519. (b) Callsen, D.; Brüne, B. *Biochemistry* **1999**, *38*, 2279−2286.

(11) (a) Pavlos, C. M.; Xu, H.; Toscano, J. P. *Curr. Top. Med. Chem.* **2005**, *5*, 637−647. (b) Pavlos, C. M.; Xu, H.; Toscano, J. P. *Free Radical Biol. Med.* **2004**, *37*, 745−752.

(12) Ford, P. C.; Bourassa, J.; Miranda, K.; Lee, B;, Lorkovic, I.; Boggs, S.; Kudo, S.; Laverman, L. *Coord. Chem. Rev.* **1998**, *171*, 185−202.

(13) (a) Ali, S. M.; Olivo, M. *Int. J. Oncol.* **2003**, *22*, 751−756. (b) Gupta, S.; Ahmad, N.; Mukhtar, H. *Cancer Res.* **1998**, *58*, 1785−1788.

(14) (a) Yamamoto, F.; Ohgari, Y.; Yamaki, N.; Kitajima, S.; Shimokawa, O.; Matsui, H.; Taketani, S. *Biochem. Biophys. Res. Commun.* **2007**, *353*, 541−546. (b) Lu, Z.; Tao, Y.; Zhou, Z.; Zhang, J.; Li, C.; Ou, L.; Zhao, B. *Free Radical Biol. Med.* **2006**, *41*, 1590−160.

(15) (a) Butler, A. R.; Megson, I. L. *Chem. Rev.* **2002**, *102*, 1155−1165. (b) Matthews, E. K.; Seaton, E. D.; Forsyth, M. J.; Humphrey, P. P. A. *Br. J. Pharmacol.* **1994**, *113*, 87−94. (c) Clarke, M. J.; Gaul, J. B. *Struct. Bonding (Berlin)* **1993**, *81*, 147−181. (d) Arnold, W. P.; Longnecker, D. E.; Epstein, R. M. *Anesthesiology* **1984**, *61*, 254−60. (e) Palmer, R. F.; Lasseter, K. C. *N. Engl. J. Med.* **1975**, *292*, 294−297.

(16) Bourassa, J.; DeGraff, W.; Kudo, S.; Wink, D. A.; Mitchell, J. B.; Ford, P. C. *J. Am. Chem. Soc.* **1997**, *119*, 2853−2860.

(17) Conrado, C. L.; Bourassa, J. L.; Egler, C.; Wecksler, S.; Ford, P. C. *Inorg. Chem.* **2003**, *42*, 2288−2293.

(18) (a) Alaniz, C.; Watts, B. *Ann. Pharmacother.* **2005**, *39*, 388−389. (b) Janczyk, A.; Wolnicka-Glubisz, A.; Chmura, A.; Elas, M.; Matuszak, Z.; Stochel, G.; Urbanska, K. *Nitric Oxide* **2004**, *10*, 42−50. (c) Bourassa, J.; Lee, B.; Bernard, S.; Schoonover, J.; Ford, P. C. *Inorg. Chem.* **1999**, *38*, 2947−2952. (d) Mayer, B.; Brunner, F.; Schmidt, K. *Biochem. Pharmacol.* **1993**, *45*, 367−374. (e) Robin, E. D.; McCauley, R. *Chest* **1992**, *102*, 1842−1845.

(19) Patra, A. K.; Afshar, R. K.; Olmstead, M. M.; Mascharak, P. K. *Angew. Chem., Int. Ed.* **2002**, *41*, 2512−2515.

(20) Patra, A. K.; Rowland, J. M.; Marlin, D. S.; Bill, E.; Olmstead, M. M.; Mascharak, P. K. *Inorg. Chem.* **2003**, *42*, 6812−6823.

(21) Patra, A. K.; Olmstead, M. M.; Mascharak, P. K. *Inorg. Chem.* **2002**, *41*, 5403−5409.

(22) Afshar, R. K.; Patra, A. K.; Olmstead, M. M.; Mascharak, P. K. *Inorg. Chem.* **2004**, *43*, 5736−5743.

(23) Eroy-Reveles, A. A.; Hoffman-Luca, C. G.; Mascharak, P. K. *Dalton Trans.* **2007**, 5268−5274.

(24) Patra, A. K.; Mascharak, P. K. *Inorg. Chem.* **2003**, *42*, 7363−7365.

(25) Patra, A. K.; Rose, M. J.; Murphy, K. A.; Olmstead, M. M.; Mascharak, P. K. *Inorg. Chem.* **2004**, *43*, 4487−4495.

(26) Rose, M. J.; Patra, A. K.; Alcid, E. A.; Olmstead, M. M.; Mascharak, P. K. *Inorg. Chem.* **2007**, *46*, 2328−2338.

(27) Rose, M. J.; Olmstead, M. M.; Mascharak, P. K. *Polyhedron* **2007**, *26*, 4713−4718.

(28) Ghosh, K.; Eroy-Reveles, A. A.; Avila, B.; Holman, T. R.; Olmstead, M. M.; Mascharak, P. K. *Inorg. Chem.* **2004**, *43*, 2988−2997.

(29) Ghosh, K.; Eroy-Reveles, A. A.; Olmstead, M. M.; Mascharak, P. K. *Inorg. Chem.* **2005**, *44*, 8469−8475.

(30) Rowland, J. M.; Olmstead, M. M.; Mascharak, P. K. *Inorg. Chem.* **2001**, *40*, 2810−2817.

(31) (a) Ford, P. C.; Laverman, L. E. *Coord. Chem. Rev.* **2005**, *249*, 391−403. (b) Ford, P. C.; Fernandez, B. O.; Lim, M. D. *Chem. Rev.* **2005**, *105*, 2439. (c) Hoshino, M.; Laverman, L.; Ford, P. C. *Coord. Chem. Rev.* **1999**, *187*, 75−102.

(32) Lim, M. D.; Lorkovic, I. M.; Ford, P. C. *J. Inorg. Biochem.* **2005**, *99*, 151−165.

(33) The {M−NO}^{n} notation used in this paper is that of Feltham and Enemark. See Enemark, J. H.; Feltham, R. D. *Coord. Chem. Rev.* **1974**, *13*, 339−406.

(34) Szundi, I.; Rose, M. J.; Sen, I.; Eroy-Reveles, A. A.; Mascharak, P. K.; Einarsdottir, O. *Photochem. Photobiol.* **2006**, *82*, 1377−1384.

(35) Tfouni, E.; Krieger, M.; McGarvey, B. R.; Franco, D. W. *Coord. Chem. Rev.* **2003**, *236*, 57−69.

(36) Serli, B.; Zangrando, E.; Gianferrara, T.; Yellowlees, L.; Alessio, E. *Coord. Chem. Rev.* **2003**, *245*, 73−83.

Scheme 1. Synthesis of $[Mn(PaPy_2Q)(NO)]ClO_4$ (**2**)

$[Mn^{II}(PaPy_2Q)(H_2O)]ClO_4$ (**4**) $\xrightarrow{NO}$ $[Mn(PaPy_2Q)(NO)]ClO_4$ (**2**)

$[Mn^{III}(PaPy_2Q)(OH)]ClO_4$ (**3**) $\xrightarrow{NO}$ $[Mn(PaPy_2Q)(NO)]ClO_4$ (**2**)

to transfer NO to enzymes such as papain,[37] cytochrome *c* oxidase,[34] and soluble guanylate cyclase.[38] In addition, **1** elicits light-dependent increases of cGMP in smooth muscle cells and vasorelaxation of rat aortic smooth muscle tissue.[38] Finally, the remarkable stability of **1** allows easy incorporation of **1** into a sol−gel matrix, resulting in a convenient, biocompatible NO releasing material that can deliver NO to selective tissues under the strict control of light.[39]

To utilize such material in PDT of skin cancer, one has to make the NO donor sensitive to near-infrared (NIR) light because light penetration through mammalian tissue is mostly limited to the 700−1100 nm region.[40,41] It is therefore desirable that the wavelength(s) of the light required for the activation of the photochemotherapeutics falls in this optical window. To make **1** more sensitive to lights of longer wavelengths, we sought further alteration of the ligand frame rather than a change of the metal center. Previously, we have shown that more extended conjugation in a similar ligand frame affords metal nitrosyls that exhibit significant red-shifts in their photobands.[25] Following that line of thought, we have now synthesized a new ligand, *N*,*N*-bis(2-pyridylmethyl)amine-*N*-ethyl-2-quinoline-2-carboxamide ($PaPy_2QH$, where H is dissociable proton), in which the pyridyl-carboxamide group of $PaPy_3H$ is replaced by a quinolyl-carboxamide moiety.

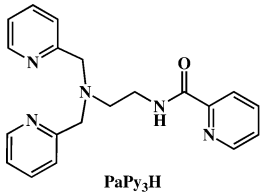

$PaPy_3H$

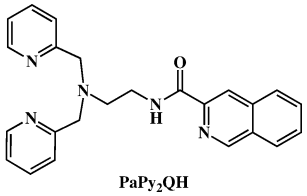

$PaPy_2QH$

In this paper, we report the synthesis, structure, and spectroscopic properties of the $\{Mn-NO\}^6$ nitrosyl $[Mn(PaPy_2Q)(NO)]ClO_4$ (**2**; Scheme 1), derived from this modified pentadentate ligand. In addition, the photochemical properties of **1** and **2** have been compared to show that **2** is truly sensitive to NIR light. To the best of our knowledge, **2** is the first metal nitrosyl that releases NO upon exposure to NIR light of low intensity (<5 mW). We also report that **2** has been encapsulated in a sol−gel matrix and the nitrosyl-polymer hybrid **2·HM** transfers NO to reduced myoglobin under NIR light (780 nm) quite readily.

Experimental Section

Quinaldic acid, 2-(chloromethyl)-pyridine hydrochloride, Mn(II) perchlorate hexahydrate, and horse heart myoglobin (Mb) were purchased from Aldrich Chemical Co. and used without further purification. Acetonitrile (MeCN), ethanol (EtOH), methanol (MeOH), and diethyl ether (Et_2O) were obtained from Fischer Chemical Co. and distilled from CaH_2, $Mg(OEt)_2$, $Mg(OMe)_2$, and sodium/benzophenone, respectively, prior to use. Triethylamine (Et_3N), ethylene diamine, and pyridine were purchased from Aldrich Chemical Co. and distilled from sodium prior to use. Nitric oxide gas was purchased from Spectra Gases and purified from higher oxides by passage through a long KOH column before use in reactions. Tecoflex SG-80A polyurethane was a gift from Noveon, Inc. Elemental analyses were performed by Desert Analytics, Inc.

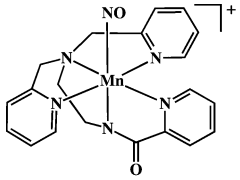

$[Mn(PaPy_3)NO]ClO_4$ (**1**)

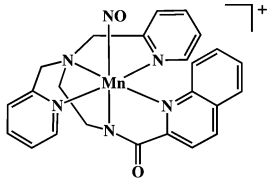

$[Mn(PaPy_2Q)NO]ClO_4$ (**2**)

Synthesis Safety Note. Transition metal perchlorates should be handled with great caution and be prepared in small quantities as metal perchlorates are hazardous and may explode upon heating.

Synthesis of the Compounds. The Mn(III) starting material $[Mn(DMF)_6](ClO_4)_3$,[42] $PaPy_3H$,[30] and $[Mn(PaPy_3)(NO)]ClO_4$[28] were synthesized by following the published procedures. All reactions were carried out in an inert N_2 atmosphere.

Ethylquinaldate. A mixture of 2.0 g (11.57 mmol) of quinaldic acid, 40 mL of EtOH, and 1.5 mL of sulfuric acid was heated to reflux for 24 h. The EtOH was then removed and the remaining solution was neutralized with 20 mL of saturated sodium bicarbonate solution. The product was extracted with 50 mL of CH_2Cl_2 and washed successively with deionized H_2O (3 × 60 mL). Next, the CH_2Cl_2 solution was dried over anhydrous $MgSO_4$ and filtered. The product was obtained as a yellow oil following removal of the solvent in vacuo (1.83 g, 85% yield). ^1H NMR (298 K, $CDCl_3$, 500 MHz, δ, ppm from TMS): 1.50 (t, 3H); 4.57 (q, 2H); 7.65 (m, 1H); 7.79 (m, 1H); 7.88 (d, 1H); 8.20 (m, 1H); 8.31 (m, 2H). ESI-MS *m*/*z* 202.09 $[M + H]^+$.

***N*-(2-Aminoethyl)-2-quinolinecarboxamide.** A mixture of 1.83 g (9.09 mmol) of ethylquinaldate, 2.73 g (45.47 mmol) of ethylenediamine, and 1.4 mL of pyridine was heated at 100 °C for 4 h. Next, the solvent was removed at reduced pressure and the remaining oil was acidified to pH 5 with concentrated HCl. The solution was washed with CH_2Cl_2 (2 × 100 mL). The aqueous layer was made basic with 30 mL of pH 10 NaOH solution and was extracted with CH_2Cl_2 (4 × 75 mL). The organic layer was then dried over anhydrous $MgSO_4$ and filtered. Removal of the solvent afforded the product as a yellow oil (1.47 g, 75% yield). ^1H NMR (298 K, $CDCl_3$, 500 MHz, δ, ppm from TMS): 1.38 (s, 2H); 3.02 (t, 2H); 3.62 (q, 2H); 7.62 (m, 1H); 7.77 (m, 1H); 7.88 (m, 1H); 8.12 (d, 1H); 8.32 (s, 2H); 8.54 (s, 1H). ESI-MS *m*/*z* 216.09 $[M + H]^+$.

***N*,*N*-Bis(2-pyridylmethyl)amine-*N*-ethyl-2-quinolinecarboxamide ($PaPy_2QH$).** A mixture of 1.47 g (6.83 mmol) of *N*-(2-aminoethyl)-2-quinolinecarboxamide, 2.24 g (13.66 mmol) of 2-(chloromethyl)-pyridine hydrochloride dissolved in 3.6 mL of deionized H_2O, and 2.8 mL of 10 M NaOH solution was stirred at 70 °C for 4 h. Then 45 mL of saturated NaOH solution was added to the mixture followed by extraction with CH_2Cl_2 until the CH_2Cl_2 layer was slightly yellow in color (4 × 75 mL). The brown solution was washed successively with an aqueous HCl solution (pH 5, 7 × 130 mL), saturated brine solution (3 × 100 mL), and 10 M NaOH solution (3 × 100 mL). Next, the CH_2Cl_2 solution was dried over anhydrous $MgSO_4$ and filtered. Removal of the solvent afforded the ligand as a dark brown oil (2.16 g, 80% yield). ^1H NMR (298 K, $CDCl_3$, 500 MHz, δ, ppm from TMS): 2.91 (t, 2H); 3.68 (q, 2H); 3.97 (s, 4H); 7.10 (m, 2H); 7.52 (m, 2H); 7.68 (m, 3H); 7.83 (m, 1H); 7.94 (m, 1H); 8.18 (d, 1H); 8.33 (q, 2H); 8.53

(37) Afshar, R. K.; Patra, A. K.; Mascharak, P. K. *J. Inorg. Biochem*. **2005**, *99*, 1458−1464.
(38) Madhani, M.; Patra, A. K.; Miller, T. W.; Eroy-Reveles, A. A.; Hobbs, A. J.; Fukuto, J. M.; Mascharak, P. K. *J. Med. Chem.* **2006**, *49*, 7325−7330.
(39) Eroy-Reveles, A. A.; Leung, Y.; Mascharak, P. K. *J. Am. Chem. Soc.* **2006**, *128*, 7166−7167.
(40) (a) Hawrysz, D. J.; Sevick-Muraca, E. M. *Neoplasia* **2000**, *2*, 388−417. (b) Anderson, R. R.; Parrish, J. A. *J. Invest. Dermatol*. **1981**, *77*, 13−19.
(41) Weissleder, R.; Ntziachristos, V. *Nat. Med.* **2003**, *9*, 123 − 128.
(42) Pravakaran, C. P.; Patel, C. C. *J. Inorg. Nucl. Chem.* **1968**, *30*, 867.

(m, 2H); 8.97 (s, 1H). Selected IR frequency (NaCl plate) $\nu_{CO} = 1660$ cm^{-1}. ESI-MS m/z 398.21 $[M + H]^+$.

[Mn(PaPy$_2$Q)(OH)]ClO$_4$·CH$_3$CN (3·CH$_3$CN). A batch of 0.112 g (1.1 mmol) of Et$_3$N was added dropwise to a solution of 0.200 g (0.5 mmol) of PaPy$_2$QH dissolved in 15 mL of MeOH and the reaction mixture was stirred for 2 h. Next, a slurry of 0.398 g (0.50 mmol) of [Mn(DMF)$_6$](ClO$_4$)$_3$ in 5 mL of MeOH was slowly added dropwise and the reaction mixture turned wine red. Finally, a batch of 20 μL (1.1 mmol) of H$_2$O was added and the solution was stored at −20 °C. After 24 h, the burgundy microcrystalline product (**3**) was collected on a sintered glass filter, washed with Et$_2$O, and dried under vacuum (0.200 g, 70% yield). Slow diffusion of Et$_2$O into a solution of **3** in CH$_3$CN afforded crystals of **3**·CH$_3$CN, which were suitable for crystallographic analysis. Anal. Calcd for C$_{26}$H$_{26}$ClMnN$_6$O$_6$ (**3**·CH$_3$CN): C, 51.29; H, 4.30; N, 13.80. Found: C, 51.34; H, 4.32; N, 13.75. Selected IR frequencies (KBr disk, cm^{-1}): 3382 (w), 1630 (vs), 1606 (s), 1566 (m), 1444 (m), 1394 (m), 1142 (m), 1086 (vs), 1023 (m), 765 (s), 636 (s), 624 (s). Electronic absorption spectrum in MeCN, λ_{max} (nm, ϵ (M^{-1} cm^{-1})): 485 (280), 740 (120); in H$_2$O, 470 (320), 800 (110). μ_{eff} (298 K, polycryst) = 4.92 μ_B.

[Mn(PaPy$_2$Q)(H$_2$O)]ClO$_4$ (4). A batch of 200 mg (0.50 mmol) PaPy$_2$QH was dissolved in EtOH (15 mL) and degassed thoroughly. Next, 15 mg (0.60 mmol) of NaH was added and the solution was stirred for 2 h. Finally, 182 mg (0.50 mmol) of [Mn(H$_2$O)$_6$](ClO$_4$)$_2$ was added as a solid to the yellow solution. Within 5 min of stirring, [Mn(PaPy$_2$Q)(H$_2$O)]ClO$_4$ precipitated out as a beige precipitate, which was collected on a sintered glass funnel and dried under vacuum for 4 h (0.150 g, 52% yield). Anal. Calcd for C$_{24}$H$_{24}$ClMnN$_5$O$_6$ (**4**): C, 50.67; H, 4.25; N, 12.31. Found: C, 50.65; H, 4.31; N, 12.28. Selected IR bands (KBr disk, cm^{-1}): 3425 (m, br), 1605 (vs), 1565 (m), 1441 (m), 1370 (s), 1330 (m), 1090 (vs), 1015 (m), 770 (m), 624 (s). X-band EPR spectrum (289 K, polycrystal): strong broad signal with $g \approx 2$.

[Mn(PaPy$_2$Q)(NO)]ClO$_4$ (2). Method A. A batch of **3** (0.100 g, 1.6 mmol) was dissolved in 20 mL of a MeCN/MeOH mixture (2:18) and thoroughly degassed. The Schlenk flask was then wrapped in Al foil and NO gas was passed over the solution for 10 min. The maroon solution was stored under NO pressure for 12 h while stirring at room temperature. Finally, the solution was placed in −20 °C for 24 h, upon which dark green crystals of [Mn(PaPy$_2$Q)(NO)]ClO$_4$ (**2**), suitable for X-ray diffraction, separated out of solution (0.050 g, 53% yield). Anal. Calcd for C$_{24}$H$_{22}$ClMnN$_6$O$_6$ (**2**): C, 49.63; H, 3.82; N, 14.47. Found: C, 49.59; H, 3.80; N, 14.51. Selected IR frequencies (KBr disk, cm^{-1}): 3427 (w), 1725 (vs), 1634 (vs), 1608 (m), 1450 (m), 1403 (m), 1096 (vs), 1028 (m), 766 (s), 622 (s). Electronic absorption spectrum in MeCN, λ_{max} (nm, ϵ (M^{-1} cm^{-1})): 240 (29500), 290 (7700), 495 (2030), 650 (420). Electronic absorption spectrum in H$_2$O, λ_{max} (nm, ϵ (M^{-1} cm^{-1})): 240 (25150), 280 (6120), 310 (5250), 500 (1725), 670 (450). ^{1}H NMR (298 K, CD$_3$CN, 500 MHz, δ, ppm from TMS): 9.37 (d, 1H), 8.55 (s, 1H), 8.10 (dd, 3H), 7.83 (s, 3H), 7.44 (s, 2H), 7.05 (s, 2H), 6.44 (s, 2H), 4.43 (d, 4H), 3.31 (s, 2H), 3.22 (s, 2H) ppm.

Method B. A batch of 15 mL of MeCN was thoroughly degassed by freeze−pump−thaw cycles. To the frozen MeCN, a batch of 0.100 g (1.6 mmol) of **4** was added and the frozen solution was allowed to warm to room temperature. Next, the Schlenk flask was covered in Al foil and NO gas was passed over the yellow slurry for 10 min until the solution turned maroon in color. The solution was stirred for 12 h. Finally, the solvent was removed by reduced pressure, and the solid was redissolved in 10 mL of a mixture of MeCN and MeOH (2:18). A portion of 15 mL of Et$_2$O was added and the mixture was stored at −20 °C for 48 h. The dark green needles were filtered and washed with Et$_2$O (0.040 g, 42% yield).

1·SG and 2·SG. We previously reported the synthesis of **1·SG** from tetraethylorthosilicate (TEOS), EtOH, H$_2$O (pH 5 with HClO$_4$), and **1**. In the present study, the method of Avnir and Kaufman was followed to prepare **1·SG** and **2·SG** without the addition of alcohol.[43] A batch of 7.5 mL of tetramethylorthosilicate (TMOS) and 4.0 mL H$_2$O was stirred for 30 min until the two-phase system formed a homogeneous solution. At this point, the TMOS solution was partitioned into four test tubes or cuvettes (2.75 mL in each) and allowed to cool to room temperature. In the dark, a batch of 2 mg of **1** or **2** was dissolved in a 300 μL mixture of H$_2$O and MeCN (1:1). The highly colored solution was added to the TMOS solution and allowed to gel in the dark. The desired transparent gel was formed within 3 h. The test tubes were then carefully broken and samples of **1·SG** or **2·SG** were collected.

2·HM. Cylinders of the nitrosyl-TMOS gel polymer **2·SG** were cut into thin slices, and the disks were coated with a solution of Tecoflex SG-80A polyurethane (2.0 g) dissolved in 20 mL of THF and dried for 30 min (in the dark). The coating process was repeated three times and the final disks of hybrid material were dried for 4 h in the dark.

1·HM was also prepared following the procedure described for **2·HM**.

X-ray Data Collection and Structure Solution and Refinement. Diffraction data for single crystals of **2** and **3** were collected at 90 K on a Bruker APEX II diffractometer. Mo Kα (0.717073 Å) radiation was used, and the data were corrected for absorption effects. The structures were solved by direct methods (SHELXS-97). All nonhydrogen atoms were refined with anisotropic displacement parameters, and hydrogen atoms were added geometrically and refined with the use of a riding model. Machine parameters, crystal data, and data collection parameters for complexes **2** and **3** are summarized in Table 1, while selected bond distances and angles are listed in Table 2. Complete crystallographic data for [Mn(PaPy$_2$Q)(NO)]ClO$_4$ (**2**) and [Mn(PaPy$_2$Q)(OH)]ClO$_4$·CH$_3$CN (**3**·CH$_3$CN) have been submitted as Supporting Information.

Other Physical Measurements. ^{1}H NMR spectra were recorded at 298 K on a Bruker 500 MHz spectrometer. Purity of the synthesized organic compounds was checked by liquid chromatography tandem mass spectrometry (LC/MS) with the aid of a Thermo Finnigan LTQ set up. Absorption spectra were recorded on a Varian Cary 50 spectrophotometer. Real-time detection of NO in solution under aerobic conditions was monitored with an *in*NO Nitric Oxide Measuring System (Innovative Instruments, Inc.) using an *ami*NO-2000 electrode.

Photochemical Experiments. Continuous-wave photolysis studies were performed using a Newport Oriel Apex Illuminator (150 W xenon

Table 1. Summary of Crystal Data, Intensity Collection, and Structural Refinement Parameters for [Mn(PaPy$_2$Q)(NO)]ClO$_4$ (**2**) and [Mn(PaPy$_2$Q)(OH)]ClO$_4$·CH$_3$CN (**3**·CH$_3$CN)

	2	**3**·CH$_3$CN
formula	C$_{25}$H$_{26}$ClMnN$_6$O$_7$	C$_{26}$H$_{26}$ClMnN$_6$O$_6$
molecular weight	612.91	608.92
cryst color, habit	red needle	light green plates
T, K	90(2)	90(2)
cryst syst	triclinic	monoclinic
space group	$P-1$	$P2_1$
a, Å	7.193(3)	8.059(2)
b, Å	14.147(6)	14.320(4)
c, Å	14.691(6)	11.900(4)
α, deg	63.558(6)	90
β, deg	77.297(6)	105.661(10)°
γ, deg	81.994(6)	90
V, Å^3	1304.4(9)	1322.3(6)
Z	2	2
d_{cald}, g cm^{-3}	1.665	1.529
abs coeff, mm^{-1}	0.856	0.654
GOF[a] on F^2	1.040	0.986
R1[b] %	0.0805	0.0393
wR2[c] %	0.1514	0.0702

[a] GOF = $[\Sigma[w(F_o^2 - F_c^2)^2]/(M - N)]^{1/2}$ (M = number of reflections, N = number of parameters refined). [b] R1 = $\Sigma\times$ef$\times$ef$F_o\times$ef $-\times$ef $F_c\times$ef$\times$ef/$\Sigma\times$ef$F_o\times$ef. [c] wR2 = $[\Sigma[w(F_o^2 - F_c^2)^2]/\Sigma[w(F_o^2)^2]]^{1/2}$.

(43) Avnir, D.; Kaufman, V. R. *J. Non-Cryst. Solids* **1987**, *192*, 180−182.

Table 2. Selected Bond Distances (Å) and Bond Angles (deg) for $[Mn(PaPy_2Q)(NO)]ClO_4$ (**2**) and $[Mn(PaPy_2Q)(OH)]ClO_4 \cdot CH_3CN$ (**3**·CH_3CN)

	2	**3**·CH_3CN
Mn-N1	2.087(3)	2.1945(19)
Mn-N2	1.956(3)	1.9680(18)
Mn-N3	2.066(3)	2.2415(19)
Mn-N4	2.062(3)	2.138(2)
Mn-N5	2.033(3)	2.171(2)
Mn-N6	1.678(3)	
Mn-O2		1.8180(16)
O2−H2		0.79(3)
N6−O2	1.237(18)	
O1−C10	1.243(4)	1.253(2)
N2−C10	1.310(5)	1.328(3)
Mn-O2−H2		116.3(19)
O2-Mn-N2		174.20(7)
Mn-N6−O2	171.5(8)	
N2-Mn-N6	174.54(13)	
N1-Mn-N2	78.88(12)	77.60(7)
N1-Mn-N3	160.08(12)	157.28(7)
N1-Mn-N4	95.45(12)	106.78(7)
N1-Mn-N5	100.54(12)	99.48(7)
N2-Mn-N3	81.83(12)	80.77(7)
N2-Mn-N4	91.69(12)	83.78(7)
N2-Mn-N5	84.99(12)	95.31(7)
N3-Mn-N4	80.15(12)	77.45(7)
N3-Mn-N5	82.56(12)	75.61(7)
N3-Mn-O2		102.60(7)
N3-Mn-N6	94.74(13)	
N4-Mn-N5	162.69(12)	152.82(7)
N4-Mn-O2		92.31(7)
N4-Mn-N6	91.91(13)	
N5-Mn-O2		90.12(7)
N5-Mn-N6	90.36(13)	

lamp) equipped with an Oriel 1/8 m Cornerstone Monochromator. The intensity of light was checked prior to each experiment with a Coherent Field Max II−T0 Laser Power Meter. Known concentrations of the samples were prepared under dim light and protected from extraneous light. All irradiations were performed under aerated conditions. Standard actinometry using Reinecke's salt was employed to calibrate the light source at various wavelengths.[44] The light intensity for the photolysis experiments ranged from 1.0×10^{-5} to 1.5×10^{-5} Ein L^{-1} s^{-1}. For quantum yield measurements, a 2.8 mM solution of **1** or **2** was prepared and placed in a 10×4 mm quartz cuvette. The absorbance along the 10 mm path was greater than 2.0 at the desired wavelength, ensuring that >99% of the incident light was absorbed. The sample was irradiated with monochromatic light (<5 mW) for defined time intervals. The photolysis was monitored by recording the electronic absorption spectrum along the 4 mm path of the cuvette at an appropriate wavelength for maximal change in the absorption spectrum. For example, aqueous solutions of **2** were monitored at 670 nm. Because the photoproduct does not exhibit any absorption in the visible region, complete loss of absorption at both 500 and 670 nm was taken as the endpoint of the photolysis (100% conversion to photoproduct).

Kinetic Studies. The rates of NO release were measured by recording the electronic absorption spectrum of **1** or **2** in MeCN and H_2O (<2 mM, 1.5 mL) and monitoring the loss of absorbance at an appropriate wavelength of samples exposed to monochromatic light (of selected wavelengths, power range 2−5 mW) for defined intervals. The plots of concentration versus time were first fitted to the three parameter exponential equation $C(t) = C_\infty + (C_0 - C_\infty)\{\exp(-k_{NO}t)\}$, where C_0 and C_∞ are the initial and final concentrations, respectively. The apparent rate constant values of NO loss (k_{NO}) were then calculated from the ln(C) versus time plot for the various NO donors.

NO Transfer to Reduced Myoglobin (Mb). All manipulations of Mb were monitored by electronic absorption spectroscopy. Reduced Mb was prepared from metMb in 20 mM phosphate buffer (pH 7.5) by addition of dithionite (~1.2 equiv). Then a pellet of **2**·**HM** was placed in the cuvette and the spectrum was taken after 10 min to ensure that Mb was still reduced. Finally, monochromatic light of 780 nm (40 mW, continuous wave diode laser, IR laser system, Intelite, Inc.) was used to illuminate the sample and transfer NO to reduced Mb.

Results and Discussion

Syntheses. In our continuing effort toward synthesis of photolabile metal nitrosyls derived from designed ligands with carboxamide groups, we have previously discovered that addition of conjugated ring systems to ligand frames often shifts the photoband of the resulting nitrosyls to a lower-energy region. For example, when the two pyridine donors of the 1,2-bis-(pyridine-2-carboxamide)-4,5-dimethylbenzene (Me_2bpbH_2) ligand are replaced with quinoline moieties, the resulting 1,2-bis-(quinaldine-2-carboxamide)-4,5-dimethylbenzene (Me_2bqbH_2) ligand affords NO complexes with red-shifted photobands. The extent of red shift of the visible bands of the metal nitrosyls with these two ligands varies with the metal center; in the case of ruthenium, $[Ru(Me_2bqb)(NO)Cl]$ exhibits its absorption band with λ_{max} at 465 nm, while analogous $[Ru(Me_2bpb)(NO)Cl]$ displays its band with λ_{max} at 400 nm.[25] A similar principle has been adopted in the design of the pentadentate ligand *N*,*N*-bis-(2-pyridylmethyl)amine-*N*-ethyl-2-quinoline-2-carboxamide ($PaPy_2QH$, H is dissociable proton) used in the present study. $PaPy_2QH$ has been synthesized in 80% yield via coupling of *N*-(2-aminoethyl)-2-quinolinecarboxamide (formed in reaction between ethylquinaldate and ethylenediamine) with 2 equiv of 2-(aminomethyl)-pyridine in H_2O (pH 10, made basic with NaOH).

The desired {Mn−NO}^{6} nitrosyl $[Mn(PaPy_2Q)(NO)]ClO_4$ (**2**) has been synthesized in two distinctly different ways. In our previous work with $PaPy_3H$ ligand, we discovered that Mn(III) complexes of the type $[Mn(PaPy_3)(B)]^+$ (where B = a basic ligand such phenolate or benzoate) undergo reductive nitrosylation[45] when reacted with excess NO and afford **1** in high yield.[29] This reactivity appears to be a general one and, indeed, the Mn(III) complex $[Mn(PaPy_2Q)(OH)]ClO_4$ (**3**) allows ready entry to the nitrosyl chemistry in the present case. Addition of $[Mn(DMF)_6](ClO_4)_3$ to a mixture of $PaPy_2QH$ and NEt_3 (1:2) in aqueous MeOH affords crystalline **3** in high yield. In this complex, the deprotonated $PaPy_2Q^-$ ligand is coordinated to the Mn(III) center along with one hydroxide (vide infra). Coordination of the deprotonated carboxamido nitrogen to the high-spin Mn(III) center ($S = 2$) in **3** is indicated by shift in the position of ν_{CO} to lower energy (1630 cm^{-1} compared to 1660 cm^{-1} for the free ligand). When purified NO gas is passed through a solution of **3** in MeCN, the purple color of the solution (λ_{max} = 485 and 740 nm) turns maroon (λ_{max} = 495 and 650 nm), which upon proper workup affords the diamagnetic {Mn−NO}^{6} nitrosyl $[Mn(PaPy_2Q)(NO)]ClO_4$ (**2**).

Complex **2** has also be synthesized from the Mn(II) complex $[Mn(PaPy_2Q)(H_2O)]ClO_4$ (**4**), which is isolated as a light tan precipitate in the reaction of $[Mn(H_2O)_6](ClO_4)_2$ and $PaPy_2Q^-$ in EtOH. Complex **4** displays a shift in ν_{CO} of the ligand to 1605 cm^{-1}, and room-temperature EPR measurements indicate

(44) (a) Murov, S. L. *Handbook of Photochemistry*; M. Dekker: New York, 1973. (b) Wegner, E. E.; Adamson, A. W. *J. Am. Chem. Soc.* **1966**, *88*, 394−404.

(45) Gwost, D.; Caulton, K. G. *Inorg. Chem.* **1973**, *12*, 2095−2099.

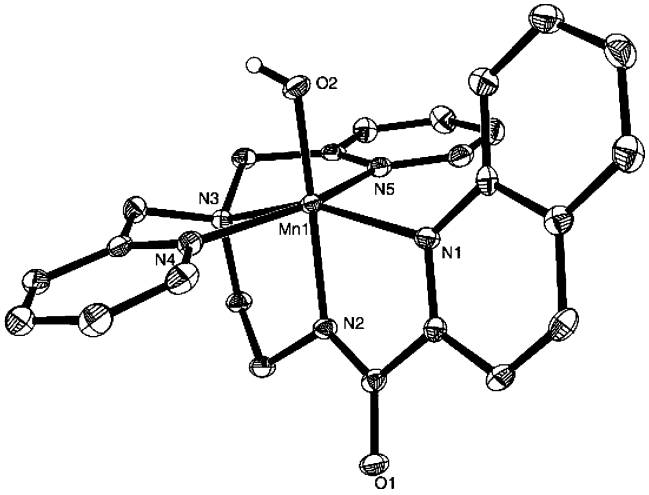

Figure 1. Thermal ellipsoid (probability level 50%) plot of $[Mn(PaPy_2Q)(OH)]^+$ (cation of **3**) showing the atom labeling scheme. All H atoms have been omitted for the sake of clarity.

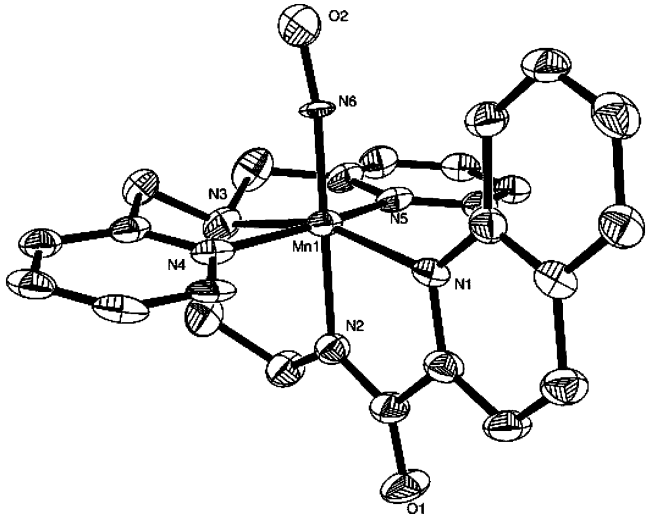

Figure 2. Thermal ellipsoid (probability level 50%) plot of $[Mn(PaPy_2Q)(NO)]^+$ (cation of **2**) showing the atom labeling scheme. All H atoms have been omitted for the sake of clarity.

that the Mn(II) center is high-spin ($S = 5/2$). Although we have not been able to determine the structure of **4**, this Mn(II) species also serves as a starting material for the synthesis of **2**. When a slurry of **4** in MeCN is exposed to purified NO gas, one obtains a clear maroon solution from which **2** can be isolated in moderate yield. In this reaction, NO simply replaces the coordinated H_2O molecule in **4** to afford **2**. Because **4** is highly sensitive to oxygen, the more stable Mn(III) complex **3** is the preferred starting material for the synthesis of **2**.

Structures of the Complexes. $[Mn(PaPy_2Q)(OH)]ClO_4 \cdot CH_3CN$ ($3 \cdot CH_3CN$). As shown in Figure 1, the Mn(III) center of **3** exists in a pseudo octahedral geometry. The *tert*-amine nitrogen, the two pyridine nitrogens, and the quinoline nitrogen of the $PaPy_2Q^-$ ligand are coordinated in the equatorial plane, while the carboxamido nitrogen and the hydroxide occupy the axial positions. The outermost ring of the quinoline moiety is positioned above the equatorial plane. The mode of binding of $PaPy_2Q^-$ to the Mn(III) center is very similar to that observed in other Mn(III) complexes of $PaPy_3^-$, such as $[Mn(PaPy_3)(OPh)]ClO_4$ (**5**).[29] Comparison of the metric parameters of **3** with **5** (both containing high-spin $S = 2$ Mn(III) centers) reveal only slight changes despite modification of the ligand frame. For example, the $Mn-N_{quin}$ distance (2.1945(19) Å) of **3** is slightly longer than the $Mn-N_{py}$ distance of **5** (2.1147(13) Å), while the other $Mn-N_{py}$ distances of **3** (average value 2.1545(2) Å) are slightly shorter than those in **5** (average value 2.2002(13) Å). The Mn−O bond distance of **3** (1.8180(6) Å) is typical for a Mn(III)−OH bond in a cationic complex, such as in the high-spin Mn(III) complex of the neutral pentadentate ligand PY5, $[Mn(PY5)(OH)](ClO_4)_2$ (Mn−O distance = 1.807(3) Å).[46]

$[Mn(PaPy_2Q)(NO)]ClO_4$ (2). In **2**, the Mn center is in a distorted octahedral environment with $PaPy_2Q^-$ coordinated in the same fashion as in **3** (Figure 2). However, the Mn−N bond distances of **2** are uniformly shorter than those of **3** due to the presence of a low-spin Mn(II) center in **2** instead of the high-spin Mn(III) center present in **3**. For example, the $Mn-N_{quin}$ and $Mn-N_{amine}$ distances of **2** are 2.087(3) and 2.066(3) Å, respectively, while the same bonds are 2.1945(19) and 2.2415(19) Å long in **3**. This same trend was noted during formation of **1** via reductive nitrosylation of **5** with NO.[29] Comparison of the metric parameters of **2** and **1** reveals that the five Mn−N(ligand) distances are similar in these two nitrosyls. The only noticeable differences between **2** and **1** exist in the Mn−N−O unit.[28] Both the Mn−N(O) and N−O distances of **2** (1.678(3) and 1.237(18) Å) are longer than the corresponding distances of **1** (1.6601(14) and 1.1918(18) Å). The slight elongation of the N−O bond is consistent with the shift in ν_{NO} observed for these two nitrosyls (1745 cm^{-1} for **1** compared to 1725 cm^{-1} for **2**). Overall, the Mn−N(O) and N−O distances of both **1** and **2** fall within the range of other manganese nitrosyls (Mn−N(O), 1.58−1.69 Å; and N−O, 1.18−1.23 Å).[47,48] Interestingly, the corresponding iron nitrosyls $[Fe(PaPy_3)NO](ClO_4)_2$ and $[Fe(PaPy_2Q)NO](ClO_4)_2$ do not exhibit such changes in the Fe−N−O unit upon change in the ligand frame.[20,23] Finally, the almost linear Mn−N6−O2 angle of **2** (171.5(8)°) is very close to that noted in **1** (171.91(13)°).[28]

Electronic Description. Complex **2** is diamagnetic both in solid state and in solution. The $S = 0$ ground state of this nitrosyl is also confirmed by its ^1H NMR spectrum in CD_3CN (prepared and run in the dark). The IR spectrum of **2** displays one strong NO stretch at 1725 cm^{-1}, a value similar to the NO stretch of **1** (1745 cm^{-1}).[28] The ν_{NO} values of both **1** and **2** fall within the range of other diamagnetic manganese nitrosyls (1700−1775 cm^{-1}).[47]

The diamagnetism of **2** indicates a strong coupling between the low-spin Mn(II) center and NO much like that observed in **1**.[28] The corresponding {Fe-NO}^{6} nitrosyls $[Fe(PaPy_3)NO](ClO_4)_2$ and $[Fe(PaPy_2Q)NO](ClO_4)_2$ are also diamagnetic with linear NO bond.[20,23] Interestingly, while the metal−N(O) distances are very similar in these four nitrosyls (range: 1.6601−1.6817 Å), significant differences exist when one compares the N−O bond distance in manganese versus iron

(46) Goldsmith, C. R.; Cole, A. P.; Stack, D. P. *J. Am. Chem. Soc.* **2005**, *127*, 9904−9912.

(47) (a) Franceschi, F.; Hesschenbrouck, J.; Solari, E.; Floriani, C.; Re, N.; Rizzoli, C.; Chiesi-Villa, A. *J. Chem. Soc., Dalton Trans.* **2000**, 593−604. (b) Cooper, D. J.; Ravenscroft, M. D.; Stotter, D. A. *J. Chem. Res. A* **1979**, 3359−3384. (c) Coleman, W. M.; Taylor, L. T. *J. Am. Chem. Soc.* **1978**, *100*, 1705−1710. (d) Cotton, F. A.; Monchamp, R. R.; Henry, R. J. M.; Young, R. C. *J. Inorg. Nucl. Chem.* **1959**, *10*, 28−38.

(48) Franz, K. J.; Lippard, S. J. *J. Am. Chem. Soc.* **1998**, *120*, 9034−9040.

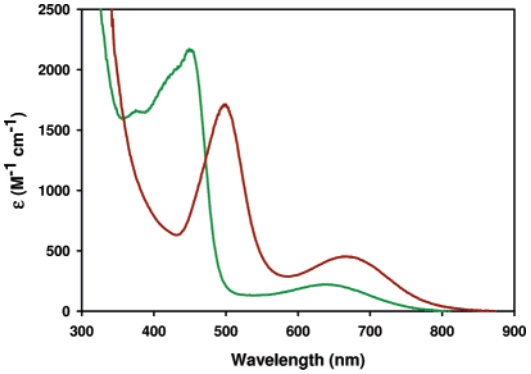

Figure 3. Comparison of the electronic absorption spectra of [Mn($PaPy_3$)(NO)]ClO_4 (**1**, green trace) and [Mn($PaPy_2Q$)(NO)]ClO_4 (**2**, maroon trace) in H_2O.

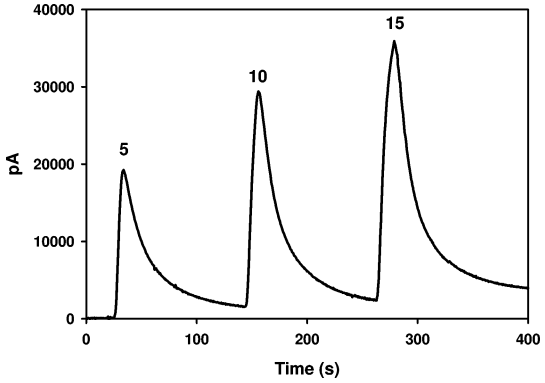

Figure 4. Chronoamperogram generated with *ami*NO-2000 electrode upon photodissociation of NO from **2** in H_2O under illumination with 810 nm light (4.23 mW). The numbers above the peaks indicate the number of seconds of illumination.

species. The N−O bond distance is ∼ 0.05 Å longer in **1** and **2** (1.1918(18) Å and 1.237(8) Å, respectively) compared to the same distance in the iron nitrosyls (1.139(3) Å and 1.1435(18) Å, respectively). This explains the lower ν_{NO} values of **1** and **2** (1745, 1725 cm^{-1}) compared to their iron analogues (1920, 1885 cm^{-1}). Based on spectroscopic evidence, we have previously assigned a low-spin Fe(II)−NO^+ formulation for the {Fe−NO}^{6} iron nitrosyls.[20,23] In contrast, the {Fe−NO}^{7} nitrosyl [Fe($PaPy_3$)NO](ClO_4), which has been assigned an Fe(II)−$NO^•$ formulation, exhibits a N−O bond distance of 1.190(2) Å.[20] This distance is much closer to the N−O bond distances noted with the manganese nitrosyls, a fact that provides further support to the Mn(II)−$NO^•$ formulation for **1** and **2**.

Franz and Lippard have recently reported a {Mn−NO}^{6} nitrosyl [Mn(NO)(TC-5,5)] derived from the dianionic tetradentate tropocoronand macrocycle TC-5,5.[48] Based on the metric and spectroscopic parameters, they have assigned a Mn(III)−O^- formulation for the {Mn−NO}^{6} core of this nitrosyl. Close scrutiny of the properties however distinguishes the present {Mn−NO}^{6} nitrosyls **1** and **2** from [Mn(NO)(TC-5,5)]. For example, [Mn(NO)(TC-5,5)] is *not diamagnetic* and its room-temperature magnetic moment (4.3 μ_B) is consistent with other high-spin Mn(III) complexes. In addition, [Mn(NO)(TC-5,5)] exhibits a considerably lower value of ν_{NO} (1662 cm^{-1}), a fact that supports its Mn(III)−NO^- description. The diamagnetic ground states and greater values of ν_{NO} (1745 and 1725 cm^{-1}) of **1** and **2** are clearly distinct and hence we formally assign both **1** and **2** as Mn(II)−$NO^•$ (instead of Mn(III)−NO^-) species.[28]

Electronic Absorption Spectrum. In MeCN, both **1** and **2** exhibit a quasireversible cyclic voltammogram with $E_{1/2} = 0.9$ V vs SCE (Figure S4, Supporting Information).[28] It therefore appears that there is little effect of the additional conjugation on the redox state of the manganese center. However, in the same solvent, the two nitrosyls dissolve to afford two distinctly different colored solutions. The green solution of **1** in MeCN exhibits its visible absorption bands with λ_{max} at 440 and 635 nm,[28] while the maroon solution of **2** in the same solvent displays bands with λ_{max} at 495 and 650 nm. In H_2O, **2** exhibits absorption bands with λ_{max} at 500 and 670 nm (Figure 3). Clearly, change in the ligand frame (from $PaPy_3^-$ to $PaPy_2Q^-$) brings about changes in the absorption parameters of **2** in the desired direction (to lower energy). In addition, the extinction coefficient of the low-energy band of **2** is enhanced to a significant extent, from 220 M^{-1} cm^{-1} (for **1**)[28] to 450 M^{-1} cm^{-1}. Similar red shift of the absorption band(s) upon change in the ligand from $PaPy_3^-$ to $PaPy_2Q^-$ has been observed in the corresponding {Fe−NO}^{6} (10 nm red shift)[23] and {Ru−NO}^{6} (10 nm red shift)[27] nitrosyls in MeCN and other solvents. The overall color change is however more dramatic in case of manganese due to greater extent of changes in the absorption spectrum (particularly the second absorption band in the 400−500 nm range, Figure 3) compared to the other two isoelectronic nitrosyls. Also, in the case of manganese, the nitrosyls exhibit significant absorption in the 600−800 nm range, a fact that renders these two nitrosyls sensitive to visible and NIR light, respectively.

NO Photolability of 1 and 2. In the solid state, **2** is stable for over 6 months when stored in the dark. No significant decomposition is noted even when the crystals are kept under room light and in air. Also, when aerobic solutions of **2** in MeCN are kept in the dark, the electronic absorption spectrum does not change appreciably, even after two weeks. However, exposure of a solution of **2** to visible light causes rapid release of NO (detected by an *ami*NO-2000 electrode) and bleaching of the dark maroon color (Figure S5, Supporting Information). We have previously reported that solutions of **1** releases NO upon exposure to *visible* light.[28] Based on results of computational studies, Richards and co-workers have assigned the photoactivity of [Fe($PaPy_3$)(NO)]$(ClO_4)_2$ to the promotion of an electron from a metal-based molecular orbital (with significant contribution from the ligated carboxamido group) to a Fe−NO π^* antibonding molecular orbital.[49] Ford and others have also assigned the photoactivity of {Ru−NO}^{6} nitrosyls to d_π(Ru) → π^*(NO) transitions.[50,51] It is now evident that the sensitivity of {M−NO}^{6} nitrosyls of this type to light depends on the specific locations of their corresponding M → π^*(NO) transitions (photobands). Both **1** and **2** display absorptions in the 500−800 nm range and, hence, exhibit excellent NO photolability when exposed to light of longer wavelengths.

Careful examination of the wavelength dependence of the photobleaching reaction of **2** reveals that this new {Mn−NO}^{6} nitrosyl is sensitive to light from UV to NIR region (300−850 nm). For example, exposure of an aqueous solution of **2** to 810 nm light (4.23 mW) elicits an immediate response of the NO specific electrode and bleaching of the maroon color. The chronoamperogram of NO detection from **2** (Figure 4) demonstrates that **2** is quite sensitive to 810 nm light and exhibits a linear on−off response to illumination. This confirms that the release of NO from **2** can be triggered by NIR light. The process

(49) Greene, S. N.; Richards, N. G. J. *Inorg. Chem.* **2004**, *43*, 7030−7041.
(50) Works, C. F.; Jocher, C. J.; Bart, G. D.; Bu, X.; Ford, P. C. *Inorg. Chem.* **2002**, *41*, 3728−3739.
(51) Gorelsky, S. I.; Lever, A. B. P. *Int. J. Quantum Chem.* **2000**, *80*, 636−645.

Table 3. Quantum Yields (Φ) for Photoreactions of [Mn($PaPy_3$)(NO)]ClO_4 (**1**) and [Mn($PaPy_2Q$)(NO)]ClO_4 (**2**)

complex	solvent	λ_{irr} (nm)	Φ (mol/einst)
1	H_2O	500	0.400 ± 0.010
1	H_2O	550	0.385 ± 0.010
2	H_2O	500	0.742 ± 0.010
2	H_2O	550	0.694 ± 0.010
1	MeCN	500	0.326 ± 0.010
1	MeCN	550	0.309 ± 0.010
2	MeCN	500	0.623 ± 0.010
2	MeCN	550	0.579 ± 0.010

of NO photorelease from **2** upon exposure to light is clean (much like **1**). The absorption spectra of photolyzed solutions of **2** (in H_2O or MeCN) display isosbestic points (at 850 nm in H_2O, at 340 and 790 nm in MeCN), indicating clean conversion of **2** into the colorless solvato Mn(II) species $[Mn(PaPy_2Q)(Solv)]^+$ (reaction 1), which exhibits a strong and broad EPR signal at $g = 2$. It must be mentioned that this process results in complete (100%) release of NO, as indicated by total loss of the two

$$[Mn(PaPy_2Q)(NO)]ClO_4\ (\mathbf{2}) \underset{NO}{\overset{NO}{\overset{h\nu}{\rightleftharpoons}}} [Mn(PaPy_2Q)(Solv)]ClO_4 \quad \text{..... (1)}$$

photobands of **2**. Passage of NO through the Mn(II) solvato species in MeCN under anaerobic conditions results in slow regeneration of the $\{Mn-NO\}^6$ nitrosyl **2**, a process that can be monitored by the growth of ν_{NO} at 1725 cm^{-1}. In aqueous solution, $[Mn(PaPy_2Q)(H_2O)]^+$ eventually decomposes into $[Mn(H_2O)_6]^{2+}$ (detected by EPR spectroscopy) and free ligand (confirmed by its NMR spectrum following extraction into $CDCl_3$) over a period of 5 days, regardless of the presence or absence of oxygen.

Quantum Yield Measurements. Quantum yield values (Φ) for the generation of NO from **1** and **2** are listed in Table 3. These values were determined from changes in the electronic absorption spectra upon exposure to light of two different wavelengths (500 and 550 nm) and in different solvents (H_2O and MeCN). The Φ values for **2** are significantly greater than the values of **1** in both solvents. This indicates that incorporation of a quinolyl-carboxamide moiety in place of the pyridyl-carboxamide group is not only effective in moving the photosensitivity to light of longer wavelengths, but also in improving Φ values of the resulting $\{Mn-NO\}^6$ nitrosyl. The iron and ruthenium nitrosyls of these two ligands also see a significant increase in photoactivity (vide infra, Table 6).

It must be mentioned here that the availability (and properties) of chemical actinometers[52] restricted our Φ value measurements to 500 and 550 nm. Inspection of Figure 3 reveals that **1** has much less absorption than **2** at these wavelengths. However, because the Φ values were measured with solutions of absorbance value of 2, the Φ values in Table 3 truly represent the efficiency of NO photorelease of these two nitrosyls. Thus, **2** is not only sensitive to NIR light (Figure 4) but also is a superior NO donor in the visible range. Unfortunately, we could not measure Φ values at wavelengths in the NIR region due to lack of appropriate actinometer.[52] However, we have measured the apparent rate of NO photorelease from these two nitrosyls at longer wavelengths and compared their efficiencies (vide infra).

(52) $K_3[Fe(C_2O_4)_3]$ operates optimally in the 250−450 nm range (see Hatchard, C. G.; Parker, C. A. *Proc. R. Soc. London* **1956**, *A235*, 518−536). Reinecke's salt $K[Cr(NH_3)_2(NCS)_4]$ is suitable for the 400−600 nm range.[44]

Table 4. Apparent Rates of NO Release (s^{-1}) from [Mn($PaPy_3$)(NO)]ClO_4 (**1**) and [Mn($PaPy_2Q$)(NO)]ClO_4 (**2**) in H_2O. Concentrations of **1** and **2** = 1.8 mM.

complex	λ_{irr} (nm)	power (mW)	$k_{NO} \times 10^{-3}$ (s^{-1})
1	380	3.90	2.9 ± 0.1
1	450	4.23	2.9 ± 0.1
1	500	3.40	0.9 ± 0.1
1	540	4.16	0.7 ± 0.1
1	635	3.78	1.3 ± 0.1
1	810	4.23	0.9 ± 0.1
2	425	3.75	4.1 ± 0.1
2	500	3.40	5.3 ± 0.2
2	575	4.50	2.3 ± 0.1
2	670	3.78	3.8 ± 0.1
2	810	4.23	3.1 ± 0.1
2	810	2.02	1.4 ± 0.1
2	810	1.03	0.9 ± 0.1
2	850	2.18	1.0 ± 0.1
2	900	2.11	0.4 ± 0.1

Table 5. Apparent Rates of NO Release (s^{-1}) from [Mn($PaPy_3$)(NO)]ClO_4 (**1**) and [Mn($PaPy_2Q$)(NO)]ClO_4 (**2**) in MeCN[a]

complex	λ_{irr} (nm)	power (mW)	$k_{NO} \times 10^{-3}$ (s^{-1})
1	450	4.23	1.5 ± 0.1
1	540	4.16	0.6 ± 0.1
1	635	3.78	0.9 ± 0.1
1	800	2.83	0.4 ± 0.1
2	500	3.40	4.5 ± 0.1
2	670	3.78	2.9 ± 0.1
2	810	4.23	1.5 ± 0.1

[a] Concentrations of **1** and **2** = 1.8 mM.

Kinetic Measurements. To establish (and compare) the NIR sensitivity of **1** and **2**, we have determined the apparent rates of NO loss (k_{NO}) under lights of selected frequencies in the 500−900 nm range. The light-induced NO loss from **1** and **2** has been monitored by recording the electronic spectrum of the samples after irradiation (at a certain wavelength) for a known period of time. The light-induced NO loss from **2** in all cases follows a pseudo-first order behavior in solvents such as H_2O and MeCN. The apparent rate of photodissociation of NO from **2** under illumination with 810 nm light is shown in Figure 5. As illustrated in the inset of Figure 5, the rate of NO release is proportional to the power of the monochromatic light (810 nm).

The k_{NO} values for **1** and **2** are listed in Tables 4 and 5, respectively. As shown in Figure 6, the variation of the k_{NO} value with the wavelength of light indicates that the rate of NO release follows the absorbance profile of **2**. For example, the largest k_{NO} values are found at the λ_{max} values of **2** (500 and 670 nm). In addition, the response of **2** to light beyond 800 nm is noteworthy. These results demonstrate that **2** is a much superior NO donor compared to **1** in the entire range of 380−900 nm. Also, both **1** and **2** release NO faster in H_2O than in MeCN, presumably due to the preference of Mn(II) for O- over N-donor ligands.

Comparison with Other Photoactive NO Donors. To date, a number of metal nitrosyls that release NO upon illumination have been reported. In most cases, NO is released only when irradiated with UV light (300−400 nm). This is particularly true with the $\{Ru-NO\}^6$ nitrosyls.[35,36] Because NO delivery to malignant sites in PDT requires susceptibility of the NO donor to visible or NIR light, various strategies have been developed to sensitize metal nitrosyls to light in the 600−900 nm region. For example, da Silva and co-workers have reported a dinuclear ruthenium complex, $[Ru(NH_3)_5(pz)Ru(bpy)_2(NO)](PF_6)_5$, in

Table 6. Quantum Yields (Φ) of NO Donors That Operate in the Visible Range

complex	solvent	λ_{irr} (nm)	Φ (mol Ein^{-1})	ref.
	Manganese Nitrosyls			
$[Mn(PaPy_3)(NO)]ClO_4$ (1)	H_2O	550	0.385	this work
$[Mn(PaPy_2Q)(NO)]ClO_4$ (2)	H_2O	550	0.742	this work
	Iron Nitrosyls			
$[Fe(PaPy_3)(NO)](ClO_4)_2$	MeCN	500	0.185	19, 23
$[Fe(PaPy_2Q)(NO)](ClO_4)_2$	MeCN	500	0.258	23
RBS	H_2O	546	0.001	16
RRS	H_2O	546	0.13	16
RSE ($[Fe(\mu\text{-}SCH_2Ph)_2(NO)_4]$)	$CHCl_3$	546	1.9×10^{-4}	55c
PPIX-RSE	$CHCl_3$	546	2.5×10^{-4}	55b
RSE ($[Fe(\mu\text{-}SCH_2Ph)_2(NO)_4]$)	$CHCl_3$	436	3.2×10^{-4}	55c
fluor-RSE	$MeCN/H_2O$	436	0.0036	56b
sodium nitroprusside (SNP)	H_2O	436	0.18	58
	Ruthenium Nitrosyls			
$[Ru(PaPy_3)(NO)](BF_4)_2$	H_2O	355	0.12	21, 27
$[Ru(PaPy_2Q)(NO)](BF_4)_2$	H_2O	355	0.20	27
$[Ru(PaPy_3)(NO)](BF_4)_2$	MeCN	410	0.050	27
$[Ru(PaPy_2Q)(NO)](BF_4)_2$	MeCN	410	0.17	27
$[Ru(Me_2bpb)(NO)(Resf)]$	DMF	500	0.05	57
$[Ru(Me_2bqb)(NO)(Resf)]$	DMF	500	0.102	57
$[Ru(NH_3)_5(pz)Ru(bpy)_2(NO)](PF_6)_5$	H_2O	532	0.025	53
	Organic NO Donors			
S-nitrosoglutathione (GSNO)	H_2O	545	0.056	59
S-nitroso-*N*-acetylpenicillamine (SNAP)	H_2O	550	0.039	60
S-nitroso-*N*-acetylcysteine (SNAC)	H_2O	550	0.128	60

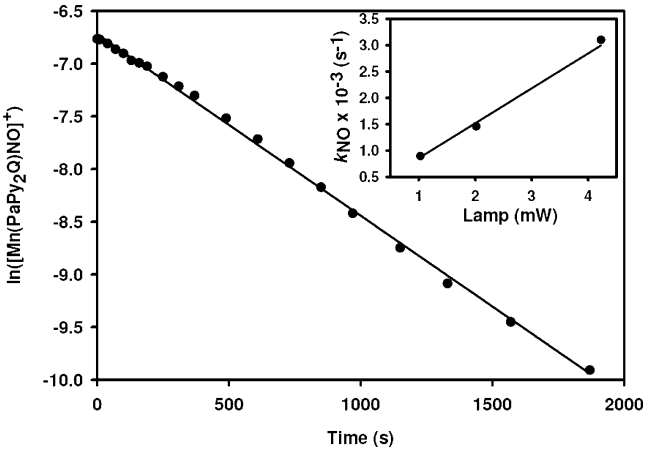

Figure 5. Plot of changes in ln([2]) vs time (s) in H_2O (as monitored by noting the absorbance at 670 nm of an aqueous solution of **2** upon illumination with 810 nm light (4.23 mW)). Inset: Plot of k_{NO} values with the power of the 810 nm light source.

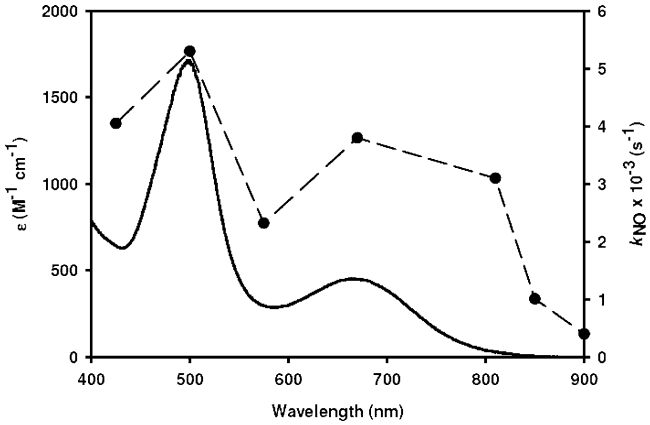

Figure 6. Electronic absorption spectrum of **2** in H_2O (solid line), k_{NO} vs λ_{irr} used during photolysis of **2** in H_2O (dashed line).

which a pyrazine (pz) bridge links $[Ru(NH_3)_5]^{2+}$ and $[Ru(bpy)_2(NO)]^{3+}$ units.[53] While $[Ru(bpy)_2(pz)(NO)]^{3+}$ is not sensitive to visible light, the dinuclear species exhibits a strong metal-to-ligand charge transfer (MLCT) absorption band of $d_\pi Ru(II) \rightarrow \pi^*(pz)$ origin in the visible region at 530 nm. As a result, this dinuclear nitrosyl releases of NO in pH 4.5 acetate buffer when exposed to 532 nm laser light (Table 6). In another attempt to sensitize a ruthenium nitrosyl to visible light, Sellman and co-workers have utilized a highly negatively charged ligand frame to shift the $d_\pi(Ru) \rightarrow \pi^*(NO)$ transition to lower energy.[54] The nitrosyl reported by this group, namely, $[Ru(NO)(py^{Si}S_4)]$-Br, releases NO under illumination with visible light (≥455 nm).[54] Ford and co-workers have utilized a different strategy, namely, attachment of strongly colored chromophores, to sensitize the metal nitrosyls. For example, the Roussin's red salt $[Fe(\mu\text{-}SCH_2Ph)_2(NO)_4]$ (RSE) has been sensitized to visible light via attachment of protoporphyrin IX (PPIX) and fluorescein.[55,56] However, insufficient energy transfer from the light-harvesting chromophores to the iron centers due to multiple methylene groups in the linkers results in minor improvement in NO releasing capacity of PPIX-RSE and Fluor-RSE conjugates (Table 6). We have recently attached the bright red dye Resorufin (Resf) *directly* to the M−NO moiety of $[Ru(Me_2bqb)(NO)Cl]$ to improve its sensitivity to visible light.[57] The

(53) Sauaia, M. G.; de Lima, R. G.; Tedesco, A. C.; da Silva, R. S. *J. Am. Chem. Soc.* **2003**, *125*, 14718−14719.
(54) Prakash, R.; Czaja, A. U.; Heinemann, F. W.; Sellman, D. *J. Am. Chem. Soc.* **2005**, *127*, 13758−13759.
(55) (a) Wecksler, S. R.; Mikhailovsky, A.; Ford, P. C. *J. Am. Chem. Soc.* **2004**, *126*, 13566−13567. (b) Conrado, C. L.; Wecksler, S.; Egler, E.; Magde, D.; Ford, P. C. *Inorg. Chem.* **2004**, *43*, 5543−5549. (c) Conrado, C. L.; Bourassa, J. L.; Egler, E.; Wecksler, S.; Ford, P. C. *Inorg. Chem.* **2003**, *42*, 2288−2293.
(56) (a) Wecksler, S. R.; Mikhailovsky, A.; Korystov, D.; Ford, P. C. *J. Am. Chem. Soc.* **2006**, *128*, 3831−3837. (b) Wecksler, S. R.; Hutchinson, J.; Ford, P. C. *Inorg. Chem.* **2006**, *45*, 1192−1200.
(57) Rose, M. J.; Olmstead, M. M.; Mascharak, P. K. *J. Am. Chem. Soc.* **2007**, *129*, 5342−5343.
(58) (a) Singh, R. J.; Hogg, N.; Neese, F.; Joseph, J.; Kalyanaraman, B. *Photochem. Photobiol.* **1995**, *61*, 325−330. (b) Wolfe, S. K.; Swinehart, J. H. *Inorg. Chem.* **1975**, *14*, 1049−1053.

dye-conjugate [Ru(Me$_2$bqb)(NO)(Resf)] exhibits a very strong absorption band at 500 nm and rapidly releases NO when exposed to visible light (Table 6). In the present work, we have adopted yet another strategy to improve the NO releasing capacity of our metal nitrosyls, namely, alteration of the ligand frame. By adding extended conjugation in the ligand frame, we have been able to move the photoband more into the NIR region. As a result, **2** is more sensitive to NIR light compared to **1**, although both are very efficient NO donor in the visible range. In Table 6, we have listed the quantum yield values of selected organic NO donors along with reported metal nitrosyls that release NO when exposed to visible light. A close look at Table 6 reveals that the NO donating capacity of **1** and **2** far exceeds that of the other nitrosyls.

In recent years, Ford and co-workers have utilized the technique of two-photon excitation (TPE) to promote NO photorelease from PPIX-RSE and Fluor-RSE via exposure to femtosecond laser pulses of NIR light (λ_{irr} = 810 nm, 210−450 mW).[55,56] This strategy is somewhat restricted by the large dependency of the technique on the photochemistry of the NO-containing species in the visible range. Also, the TPE technique requires ultrafast pulses of laser light to cause the simultaneous two-photon absorption required for NO photorelease. Illumination with lower-intensity light (<200 mW) does not release NO (as detected by an NO electrode) from PPIX-RSE and Fluor-RSE. Quite in contrast, **2** releases NO upon single photon excitation and hence can be triggered by simple exposure to NIR light (<5 mW).

Immobilization of 1 and 2 in Porous Material. To deliver NO *at selected targets under the total control of NIR light*, we have immobilized **2** in a silica-based porous material via sol−gel chemistry. When a mixture of an aqueous solution of **2** and tetramethylorthosilicate (TMOS) is allowed to gel for 3 h in the dark, an optically transparent maroon sol−gel, **2·SG**, is obtained. The electronic absorption spectrum of **2·SG** is identical to that of **2** in H_2O, a fact that confirms that the manganese nitrosyl survives the gelation process. Also, the sol−gel entrapment/occlusion process does not change the ability of **2** to release NO. When **2·SG** is exposed to light, the color of the maroon gel bleaches to faint pink (indicating formation of the photoproduct [Mn(PaPy$_2$Q)(H_2O)]ClO_4) and a steady release of NO is detected. As shown in Figure 7, **2·SG** exhibits excellent spatial differentiation when selectively irradiated with light. The sharp contrast between illuminated (faint pink) and nonilluminated (maroon) areas demonstrates that careful delivery of light will result in precise spatial release of NO by **2·SG**.

The light-induced NO loss from **2·SG** can be monitored by recording the electronic spectrum of the optically transparent samples. Photolysis of NO from **2·SG** follows a pseudo-first order behavior, similar to **2** in solution. This behavior mirrors that reported of **1·SG** under illumination.[39] Comparison of the apparent rate of NO loss (k_{NO}) between these two materials (Table 7) indicates the k_{NO} values of **2·SG** are much larger than **1·SG**, again reflecting the behavior of the free nitrosyls in solution.[61] These values demonstrate that **2·SG** is a superior NO donating material than **1·SG**. In addition, the NIR sensitivity is retained in **2·SG** (Table 7).

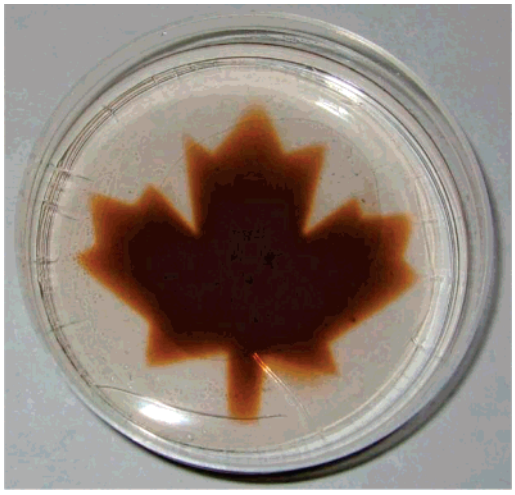

Figure 7. Selective irradiation of a circular slice of **2·SG** with a black plastic maple leaf on top. The nonirradiated area is maroon, while the photolyzed area is colorless. Light source: 25 W tungsten bulb.

Table 7. Apparent Rates of NO Release (s^{-1}) from **1·SG** and **2·SG**[a]

complex	λ_{irr} (nm)	power (mW)	$k_{NO} \times 10^{-3}$ (s^{-1})
1·SG	450	4.23	4.5 ± 0.5
1·SG	810	4.23	1.5 ± 0.1
2·SG	500	3.40	12.6 ± 0.5
2·SG	810	4.23	5.6 ± 0.1

[a] Concentration of **1** or **2** in nitrosyl sol−gel hybrid = 1.8 mM.

The rapid photorelease of NO from **1·SG** and **2·SG** raised the question regarding the ease with which the NO-depleted material could be regenerated. It is encouraging to note that **1·SG** can be regenerated by simply exposing the NO-depleted material to NO under anaerobic conditions. The regeneration process can be followed visually, because the yellow photolyzed material turns deep green when placed under NO. The completion of the process, checked by monitoring the growth of the 635 nm band, usually takes 24 h. The ability to regenerate a NO donating material upon exposure to NO gas has been noted in materials incorporating diazeniumdiolates and ruthenium nitrosyls by other groups.[9,62,63] Unfortunately, such regeneration has not been possible for **2·SG** due to the inherent instability of [Mn(PaPy$_2$Q)(Solv)]ClO_4, the photoproduct of **2**, in aqueous environments such as in the water-containing sol−gel material. This fact is also responsible for the reduced shelf life of **2·SG** compared to **1·SG**. For instance, **1·SG** can be stored in the dark for many weeks (as indicated by its electronic spectrum), while the color of **2·SG** starts to fade after 2 days.[64]

Because the nitrosyl compounds are not covalently attached to the silicate framework of the sol−gel material in **1·SG** and

(59) Sexton, D. J.; Muruganandam, A.; McKenney, D. J.; Mutus, B. *Photochem. Photobiol.* **1994**, *59*, 463−467.
(60) Singh, R. J.; Hogg, N.; Joseph, J.; Kalyanaraman, B. *FEBS Lett.* **1995**, *360*, 47−51.

(61) The apparent rates of NO release from **1·SG** and **2·SG** (Table 7) are much faster than **1** and **2** in water (Table 4) due to immobilization of the nitrosyls in the polymeric matrix. The light beam from the monochromator only illuminates a small section of the cuvette containing **1·SG** or **2·SG** and no stirring of the medium is possible. As a result, the light-exposed area is not replenished by a fresh supply of the nitrosyl complex. The apparent rate law calculation therefore affords a higher value of k_{NO} in case of the nitrosyl sol−gel hybrids.

(62) Mitchell-Koch, J. T.; Reed, T. M.; Borovik, A. S. *Angew. Chem., Int. Ed.* **2004**, *43*, 2806−2809.
(63) Ferreira, K. Q.; Schneider, J. F.; Nascente, P. A. P.; Rodrigues-Filho, U. P.; Tfouni, E. *J. Colloid Interface Sci.* **2006**, *300*, 543−552.

(64) This behavior parallels the behavior of the nitrosyls in aqueous solution. While aqueous solutions of **1** can be kept intact for weeks at room temperature, solutions of **2** are stable for several hours and decomposes significantly (~40%) within 24 h.

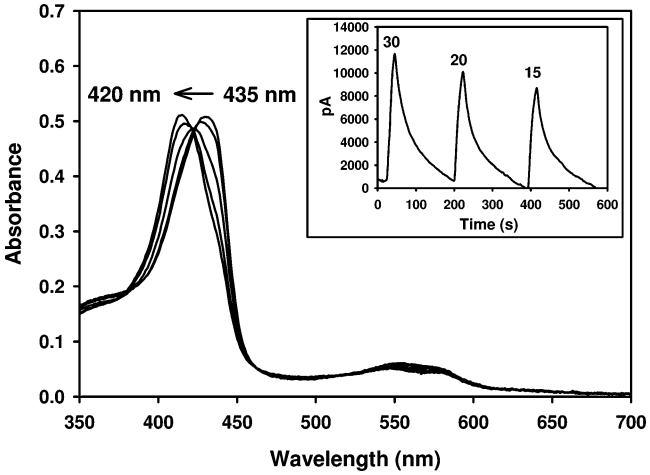

Figure 8. Transfer of NO from **2·HM** to reduced Mb (λ_{max} = 435 nm), resulting in the Mb−NO adduct (λ_{max} = 420 nm) in pH 7.5 phosphate buffer with 780 nm light (40 mW continuous wave diode laser, spectra collected at 20 s intervals of illumination). Inset: NO chronoamperogram showing NO photorelease from **2·HM** in H_2O upon illumination with 810 nm light. The numbers above peaks indicate the number of seconds of illumination.

2·SG, one needs to worry about leakage of the nitrosyls and their photoproducts in solution. In general, when TMOS is used in the sol−gel formulation instead of tetraethylorthosilicate (TEOS), the gelation time is much shorter (a few hours instead of a few days) and the sol−gel polymer is more cross-linked (and, hence, less porous). This results in less leakage of the nitrosyls into the surrounding solutions (<5% for the TMOS gel compared to 10% for the TEOS gel over 24 h, as measured by their absorption spectra). Previously, we have circumvented this problem of leaching by coating **1·SG** (prepared via TEOS gelation) with polyurethane to completely seal **1** inside the hybrid material **1·HM** (HM = hybrid material, sol−gel + polyurethane).[39] Polyurethanes are widely used in medical devices due to their excellent biocompatibility[65] and have been shown to improve the stability of materials by preventing the leakage of toxic compounds.[66] In the present work, we have formulated both **1·SG** and **2·SG** with TMOS and then dip-coated the materials in THF solutions of dissolved polyurethane to effectively *lock* the nitrosyls inside the material. That NO permeates the polyurethane coat of both **1·HM** and **2·HM** is readily confirmed by the immediate response of the NO-specific electrode when these materials are exposed to visible light. The chronoamperogram of NO photoreleased from **2·HM** upon exposure to 810 nm light, shown in the inset of Figure 8, also demonstrates that **2·HM** exhibits a linear on−off response to NIR irradiation.

NO Transfer to Biological Target with NIR Light. The utility of **2·HM** has been evaluated through delivery of NO to a biological target, myoglobin (Mb), with NIR light. Because Mb readily reacts with NO, it has been suggested that Mb plays a role in NO homeostasis in the vasculature and in red muscle cells.[67] When a pellet of **2·HM** was placed inside a cuvette containing a sample of reduced Mb (λ_{max} = 435 nm) in the dark, there was no change in optical spectrum of Mb. However, when the cuvette was exposed to 780 nm light (40 mW NIR laser), NO was smoothly transferred from **2·HM** to Mb (λ_{max} = 420 nm) in a light-dependent manner, as illustrated in Figure 8. The success in NO delivery to Mb by **2·HM** opens up the possibility of using this material to promote NO-induced apoptosis in skin cancer cell lines. Such experiments are currently in progress in this laboratory.

Comparison with Other Light-Activated NO Donating Materials. Prolonged exposure to NO at elevated concentrations can result in severe side effects to the vascular system, thus limiting the therapeutic potential of systemic NO donors. To localize the release of NO, various materials have been developed that incorporate NO donors to restrict the release of NO to target cells in their immediate vicinity. Currently most reports of materials that release NO when exposed to visible light utilize *S*-nitrosothiols,[68] which are known to decompose and release NO when exposed to light.[69] Etchenique and co-workers have shown photorelease of NO from monolayers of nitrosated dithiothreitol attached to gold surfaces with a tungsten lamp (30 W).[70] Meyerhoff and co-workers have developed a trilayer silicone rubber film utilizing SNAP-derivatized fumed silica to prevent leaching of the NO donor and reaction byproducts, and this material exhibits light-dependent release of NO upon exposure to visible light (40−100 W tungsten lamps).[71] The low extinction coefficients and quantum yields (Table 6) of *S*-nitrosothiols in the visible range are often counteracted by means of a high power laser source or by increasing the irradiation time. In recent years, metal nitrosyls have also been used as immobilized NO donors because the NO delivery from nitrosyl complexes can be tuned photochemically via a variety of strategies mentioned earlier. Borovik and co-workers have developed a polymerizable styrene-modified salen ligand for covalent attachment of metal complexes to a porous organic material.[72a] The Co(II) adduct of this material displayed a higher affinity for NO over other gases (such as O_2 and CO), but removal of NO proved to be difficult.[72b] However, when the ruthenium nitrosyl was incorporated in the material, NO was rapidly released upon exposure to UV light.[62] Tfouni and co-workers have also entrapped various ruthenium nitrosyls in a silica matrix by sol−gel chemistry that release NO when illuminated with UV light.[63,73] In a recent report, da Silva and co-workers have utilized intense visible light (three 250 W tungsten bulbs) to release NO from a Ru−terpy complex immobilized in a sol−gel material to show the vasodilatory effects of NO on rat aortic rings.[74] The majority of metal nitrosyls incorporated into polymeric materials are {Ru−NO}^{6}

(65) (a) *Advances in Biomaterials*; Lee, S. M., Ed.; CRC Press: Palo Alto, 1987. (b) Lelah, M. D.; Cooper, S. L. *Polyurethanes in Medicine*; CRC Press: Boca Raton, 1986.
(66) (a) Nablo, B. J.; Schoenfisch, M. H. *Biomaterials* **2005**, *26*, 4405−4415. (b) Zhang, H.; Annich, G. M.; Miskulin, J.; Stankiewicz, K.; Osterholzer, K.; Merz, S. I.; Bartlett, R. H.; Meyerhoff, M. E. *J. Am. Chem. Soc.* **2003**, *125*, 5015−5024.
(67) (a) Moller, J. K. S.; Skibsted, L. H. *Chem. Rev.* **2002**, *102*, 1167−1178. (b) Andriambeloson, E.; Wittig, P. K. *Redox Rep.* **2002**, *7*, 131−136. (c) Wittig, P. K.; Douglas, D. J.; Mauk, A. G. *J. Biol. Chem.* **2001**, *276*, 3991−3998.
(68) Frost, M. C.; Reynolds, M. M.; Meyerhoff, M. E. *Biomaterials* **2005**, *26*, 1685−1693.
(69) (a) Williams, D. L. H. *Acc. Chem. Res.* **1999**, *32*, 869−876. (b) Butler, A. R.; Rhodes, P. *Anal. Biochem.* **1997**, *249*, 1−9.
(70) Etchenique, R.; Furman, M.; Olabe, J. A. *J. Am. Chem. Soc.* **2000**, *122*, 3967−3968.
(71) Reynolds, M. M.; Frost, M. C.; Meyerhoff, M. E. *Free Radical Biol. Med.* **2004**, *37*, 926−936.
(72) (a) Welbes, L. L.; Borovik, A. S. *Acc. Chem. Res.* **2005**, *38*, 765−777. (b) Padden, K. M.; Krebs, J. F.; MacBeth, C. E.; Scarrow, R. C.; Borovik, A. S. *J. Am. Chem. Soc.* **2001**, *123*, 1072−1079.
(73) Bordini, J.; Ford, P. C.; Tfouni, E. *Chem. Commun.* **2005**, 4169−4171.
(74) de Lima, R. G.; Sauaia, M. G.; Ferezin, C.; Pepe, I. M.; Jose, N. M.; Bendhack, L. M.; da Rocha, Z. N.; da Silva, R. *Polyhedron* **2007**, *26*, 4620−4624.

nitrosyls due to their inherent thermal stability. The two nitrosyl-polymer hybrids, **1·HM** and **2·HM**, however, utilize $\{Mn-NO\}^6$ nitrosyls that exhibit excellent stability and NO donating capacities in biological systems. These materials are notable for their capacity to photorelease NO under lights of low-intensity (usually in mWs). In addition, **2·HM** is sensitive to NIR light. The results of the present work thus demonstrate the utility of the ligand-modification strategy to isolate new and improved photosensitive nitrosyls (and materials) that could act as efficient NO donors in the visible or NIR range. The total amount of NO released from **1·HM** and **2·HM** can be easily adjusted by (i) changing the concentration of the nitrosyls in the polymer matrix, (ii) varying the thickness of the polymer disk, and/or (iii) modulating the intensity of the light used in photolysis.

Summary and Conclusions

The following are the summary and conclusions of this study.

(a) The second generation $\{Mn-NO\}^6$ nitrosyl $[Mn(PaPy_2Q)(NO)]ClO_4$ (**2**) has been synthesized and characterized by X-ray crystallography. The metric parameters of **2** have been compared with those of the first generation $\{Mn-NO\}^6$ nitrosyl $[Mn(PaPy_3)(NO)]ClO_4$ (**1**), reported by us previously. In addition, the synthesis and structure of a starting material for **2**, namely, $[Mn(PaPy_2Q)(OH)]ClO_4$ (**3**), have also been completed.

(b) The electronic absorption and photochemical properties of **2** and **1** have been investigated thoroughly to determine the effects of the ligand frames on the photorelease of NO from these two photoactive nitrosyls. Incorporation of more conjugation into the $PaPy_3H$ ligand frame (of **1**) via replacement of a pyridine moiety with a quinoline (in **2**) red shifts the absorption maxima of **2** and increases the extinction coefficient of the lower energy band. Modification of the ligand frame has doubled the NO releasing capacity of **2** (in comparison to **1**) under visible light (500−650 nm) of low-intensity (5−50 mW). The quantum yield (Φ) of **2** (0.742 ± 0.010, $\lambda_{irr} = 500$ nm, solvent: H_2O) is the largest of all Φ values of photosensitive metal nitrosyls reported so far. Even more noteworthy is the fact that **2** is sensitive to low-intensity, continuous NIR light (800−900 nm). No TPE was required to elicit its NIR sensitivity.

(c) To date, research on light-activated NO donors has been almost exclusively focused on iron and ruthenium nitrosyls in addition to *S*-nitrosothiols. Our results now establish that properly designed manganese nitrosyls can also deliver NO under light and their photoactivity can be modulated by alterations in the ligand frame.

(d) Both **1** and **2** have been immobilized in sol−gel matrices to afford **1·SG** and **2·SG**. These materials have been coated with polyurethane to generate biocompatible hybrid materials **1·HM** and **2·HM**. Both these nitrosyl-polymer hybrids deliver NO to Mb upon exposure to visible light. In addition, NO transfer to Mb has been achieved by **2·HM** under NIR light (780 nm). Such controlled release of NO to biological targets could be exploited in PDT of skin cancer.

Acknowledgment. Financial support from the NSF Grant CHE-0553405 is gratefully acknowledged. A.A.E.-R. and Y.L, were supported by NIH IMSD Grant No. GM58903.

Supporting Information Available: LC-MS of ethylquinaldate, *N*-(2-aminoethyl)-2-quinolinecarboxamide, and *N*,*N*-bis-(2-pyridylmethyl)amine-*N*-ethyl-2-quinolinecarboxamide ($PaPy_2QH$) (Figures S1−S3), cyclic voltammogram of **2** in MeCN (Figure S4), electronic absorption (800−300 nm) spectra showing photodissociation of NO from **2** in MeCN under aerobic conditions (Figure S5), X-ray crystallographic data (in CIF format), and tables for the structure determination of $[Mn(PaPy_2Q)(NO)]ClO_4$ (**2**) and $[Mn(PaPy_2Q)(OH)]ClO_4{\cdot}CH_3CN$ (**3**·CH_3CN). This material is available free of charge via the Internet at http://pubs.acs.org.

JA710265J